Estuarine, Coastal and Shelf Science (1986) **22**, 45–62

Ebb-tidal Jets: A Model of Suspended Sediment and Mass Transport at Tidal Inlets

Emin Özsoy[a]

Coastal and Oceanographic Engineering Laboratory, University of Florida, Gainesville, Florida 32611, U.S.A.

Received 23 July 1984 and in revised form 11 December 1984

Keywords: tidal inlets; tidal deltas; suspended sediments; mass transport; turbulence; jets; mixing; entrainment

Mass transport by turbulent jets issuing from tidal inlets is investigated through a model that includes lateral mixing and entrainment, bottom friction, bathymetric changes, settling rate of particles (size), possible deposition/erosion at the bottom and ambient currents and concentrations. The bottom frictional jet becomes diluted more slowly than a classical jet. A non-vanishing concentration may result offshore and a maximum may occur in the core. The concentration of a jet on a sloping bottom decreases more rapidly due to increased dilution by entrainment. The effects of bottom friction and bottom slope compete in determining the jet concentration. Deposition to the bottom occurs within the jet mainly on both sides of the centre-line, and at lower rates on the centre-line. Erosion or deposition may occur at the jet core depending on the inlet flow conditions. In the case of erosion at the core, the material extracted is deposited on the margins and the offshore areas. Sorting of the sediments is expected, with coarser materials mainly deposited in the marginal areas, while the finer sediments are more uniformly distributed and jetted further offshore. The main features of the model are verified through a limited set of observations. The qualitative agreement is enhanced for micro- and meso-tidal inlets that are dominated by tidal hydraulics.

Introduction

The attention given to tidal inlet environments is much deserved since these transition regions between inland waters and the ocean influence navigation, interior water quality, morphological changes and land development to a large extent. Due to this transition character of their hydromechanic regimes, many of the problems associated with tidal inlets remain unresolved, preventing reliable engineering decisions (Bruun, 1978).

Tidal inlets are known to be efficient sand trappers and the sediments supplied by the littoral system or by inland sources are often stored in the form of massive bars and local shoals. The equilibrium morphology that is typical of micro- or meso-tidal estuaries results mainly from the transport and subsequent deposition of sediments by the residual tidal currents (Dean & Walton, 1975; Hayes & Kana, 1976), often modified by the wave climate and freshwater inputs (Oertel, 1975; Wright & Sonu, 1975; Sonu & Wright, 1975).

The ebb-flow on the seaward side of a tidal inlet often occurs as an unsteady turbulent

[a]Present address: Institute of Marine Sciences, Middle East Technical University, P.K. 28 Erdemli, İçel, Turkey.

0272–7714/86/010045+18 $03.00/0

jet, while the flood-flow converges towards the entrance radially, and can thus be modelled as a sink-flow (French, 1960; Dean & Walton, 1975; Özsoy, 1977; Özsoy & Ünlüata; 1982). The sediments jetted offshore and deposited in the marginal shoals are therefore relatively undisturbed by the weak offshore flood velocities. Along the adjoining coasts, entrainment into the ebb-tidal jet and the converging flood-flow combine to yield a net residual transport toward the inlet entrance at all times which is often responsible for stripping the adjacent beaches of sand (Dean & Walton, 1975). The morphological evolution and the stability of tidal inlets therefore largely depend on the existing tidal exchange and sedimentation (O'Brien & Dean, 1972; Hayes & Kana, 1976). The deposition patterns are often influenced by the ebb-tidal jet, especially in the case of smaller inlets, being characterized by marginal bars extending in the offshore direction. Such elongated bars neighbouring the inlet mouth are characteristic of coasts receiving low amounts of wave energy (such as the Gulf coast of Florida), where the primary transport mechanism is tidal. On high energy coasts, wave-induced transport limits the shoal volumes; and crescentic bars encircling the inlet are more frequently observed (Oertel, 1975; Dean & Walton, 1975).

Another important problem associated with tidal inlets occurs in assessing the influence of the inlet on tidal flushing of the interior waters. An efficient mechanism contributing to flushing is the mixing and circulation in interior waters and freshwater influxes (Wang & Connor, 1975; Officer, 1976). However, less attention has been given to the role of tidal exchange through inlets, and only approximate models (other than numerical) such as that given by Taylor & Dean (1974) are available. This method is also based on the schematization of the ebb and flood flow patterns as a turbulent jet and sink-flow during the respective tidal phases. Although the unsteady features of the exchange are schematized by reducing the flow to two steady phases, this model reproduces an efficient flushing mechanism in which only a small proportion of the initial jet concentration issuing out is returned to the interior waters during the following sink (flood) flow. The evaluation of flushing or dilution coefficients through this method requires an accurate description of jet concentration in the ebb-tidal phase, but the description provided by Taylor & Dean (1974) is insufficient due to excessive simplifications. A more elaborate model for predicting flushing characteristics based on a combination of the jet model with tidal hydraulics was used by Özsoy (1977), partially presented in Mehta & Özsoy (1978).

In the present paper, the concentration diffusion in ebb-tidal jets will be investigated for both conservative and non-conservative constituents, or specifically for the cases of conservative pollutants and suspended sediments influenced by gravitational settling. In a previous article, Özsoy & Ünlüata (1982; hereforth referred to as P1) have given an analysis of the hydrodynamics of ebb-tidal jets in the near field of an inlet mouth. Here the diffusion and diffusion/settling processes within the jet will be studied based on the results of P1.

An in-depth discussion of the effects of bottom friction, topographic changes, entrainment and cross-currents, and a review of the influences of rotation, stratification and unsteady features have been given in P1. Experimental verifications of the solutions are provided by Özsoy (1977) and Mehta & Zeh (1980), indicating agreement with most of the expected features of solution in P1. The circulations induced in the outer domain of the ebb-tidal jet through entrainment velocities have been analysed by Taylor & Joshi (1979) and Joshi & Taylor (1983) under different conditions, including geometrical constraints.

The solution technique utilized in the analyses of the hydrodynamical behaviour of tidal jets (P1) has been based on the self-similarity hypothesis, and the similarity profiles of Abramovich (1963) and Stolzenbach & Harleman (1971) have been adopted. Without *a priori* assumption of similarity, Joshi (1982) has obtained the similarity requirements and found a sech-squared similarity function based upon Prandtl's hypothesis. His similarity requirements are identical to the integral mass and momentum conservation used in P1, and therefore identical solutions were obtained apart from the similarity profile. However, neither the validity of Prandtl's hypothesis nor the shape function can equally be justified for variable depth frictional jets without experiments. Furthermore, with suitable selection of the cross-stream length scale (for example, as the lateral distance at which the velocity decreases to 5% of its centre-line value), it can be shown that the hyperbolic profile does not differ significantly from that used in P1, which was the motive of Abramovich (1963) in adopting the latter.

In this paper, the analyses are extended to the jet diffusion as applied to tidal inlets with attention fixed on the simplest processes of importance. A depth-averaged model is developed as in P1; the dependence of the analytical solutions to various parameters and possible applications are discussed. Qualitative comparisons with observations are also provided.

Modelling of diffusion/settling in jets

Consider the turbulent jet produced in the ebbing phase of a tidal flow through an inlet, the solution for which has been given in P1. A model can be developed for describing the diffusion of material concentrations which may originate at the inlet or may be present in the ambient waters. A simplified depth averaged model is:

$$\frac{\partial}{\partial x}(huc)+\frac{\partial}{\partial y}(huc)=-S+\frac{\partial}{\partial y}\mathcal{J}_y, \tag{1}$$

where h is depth, u,v the velocity components (cf. Figure 1, P1), c the depth-averaged concentration, S a loss term due to settling, and $\mathcal{J}_y$ the turbulent flux of concentration

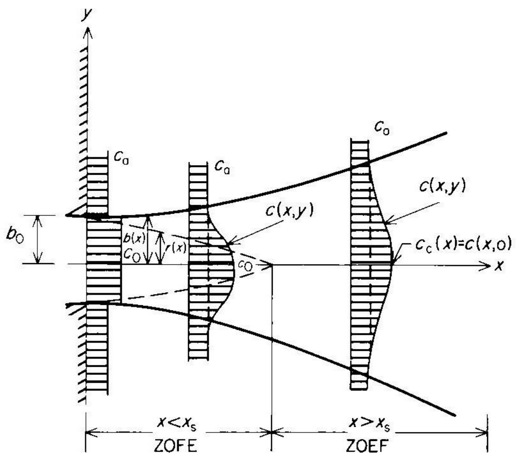

Figure 1. Definition sketch for depth-averaged diffusion in a tidal jet.

perpendicular to the jet axis. Note that the jet is assumed to be a steady one (since tidal excursion length is much larger than the inlet width) and that the diffusive/dispersive fluxes in the lengthwise direction of the jet have been neglected, consistent with the scale analyses given in P1 (see Appendix). When $S=0$, eqn (1) reduces to the diffusion equation for an ordinary 2-D jet (Abramovich, 1963; Schlichting, 1968).

The sink term in eqn (1) is to model the settling losses when c represents the average concentration of suspended sediments in the water column. In general, it is very difficult to express settling losses in a depth-averaged model such as the present one, and a certain degree of guidance is needed from empirical studies. Such studies as Odd & Owen (1972), Ariathurai & Krone (1976) and Cormault (1971), as well as the modelling approach employed by Nihoul & Adam (1975), require S to be proportional to the difference between the bottom shear stress τ^b and a critical value τ^b_{cr}:

$$S=-k(\tau^b-\tau^b_{cr}), \tag{2}$$

where k is a proportionality constant. In the jet flow (Appendix, P1), $\tau^b \simeq \tau^b_x=(\rho f/8)u^2$, and if we require $S=w_s c$ for quiescent water ($u=0$), eqn (2) reduces to:

$$S=w_s c\left(1-\frac{u^2}{u^2_{cr}}\right), \tag{3}$$

with the constant k being replaced by the appropriate value. w_s is the settling velocity of the suspended sediment and is dependent on the size of particles. Although w_s may also depend on concentration (Ariathurai & Krone, 1976) and type of bottom roughness (Cormault, 1971), some concensus exists on using eqn (3) as a model for sediment brought into suspension (erosion), when $u>u_{cr}$ ($S<0$), to be comparable to the settling to the bottom (deposition), when $u<u_{cr}$ ($S>0$). In spite of these shortcomings, the present model will be utilized here due to its relative ease of handling and in the absence of more refined empirical relations. Later, it will be shown that the choice of eqn (3) in modelling sediment transport does not significantly affect the qualitative agreement of the results with observations. In modelling passive concentrations it is sufficient to take $w_s=0$.

The velocity field u,v entering eqn (1) is to be obtained from solutions in P1. First we allow an ambient concentration $c_a=c_a(x)$ which is variable along the jet. The concentration distribution within the jet which is in excess of the ambient is assumed to be self-similar with respect to the normalized coordinate $\zeta=|y|/b(x)$:

$$\frac{c-c_a(x)}{c_c-c_a(x)}\equiv G(\zeta)=F^{1/2}(\zeta)=\begin{cases}0 \; ; & 1>\bar{\zeta}\\ 1-\bar{\zeta}^{1\cdot 5}; & 0<\bar{\zeta}<1,\\ 1 \; ; & \bar{\zeta}<0\end{cases} \qquad \bar{\zeta}=\frac{\zeta-r/b}{1-r/b}, \tag{4}$$

where $b(x)$ is the jet half-width and c_c the concentration at the jet centre-line (Figure 1; cf. P1). The similarity function $G(\zeta)$ is related to the velocity profile $F(\zeta)$ as in eqn (4), since the eddy diffusivity of scalar concentration is assumed to be twice that of momentum in turbulent jets (Abramovich, 1963; Schlichting, 1968; Stolzenbach & Harleman, 1971). The jet is separated into a *zone of established flow* ($x>x_s$, ZOEF) and a *zone of flow establishment* ($x<x_s$, ZOFE) as in P1. In the ZOFE (Fig. 1) the half-width of the core is given by $r(x)$. With the similarity hypothesis (4), eqn (1) can be integrated across the jet. As $y\rightarrow b$ the velocity u and the lateral diffusive flux $\mathcal{J}_y$ have to vanish and a lateral

entrainment velocity v_e exists related to the centre-line velocity u_c as $v_e = au_c$ and is given as $a = a_1 = 0{\cdot}036$ in the ZOFE and $a = a_2 = 0{\cdot}050$ in the ZOEF (cf. P1). In P1 [eqs 3(a–f)] we had the normalized variables:

$$\xi = \frac{x}{b_0},\ \mu = \frac{fb_0}{8h_0},\ H(\xi) = \frac{h}{h_0},\ R(\xi) = \frac{r}{b_0},\ B(\xi) = \frac{b}{b_0},\ U(\xi) = \frac{u_c}{u_0}, \qquad [5(a–f)]$$

in addition to which, the following are defined:

$$\gamma = \frac{w_s b_0}{u_0 h_0},\quad \psi = \frac{u_0}{u_{cr}},\quad C(\xi) = \frac{c_c}{c_0},\quad C_A(\xi) = \frac{c_a}{c_0}, \qquad [5(g–j)]$$

where c_0 is the concentration at the inlet mouth. The integration of eqn (1) across the jet yields:

$$\frac{d}{d\xi}(\bar{I}_4 HBUC) - aC_A HU = -\gamma BC(\bar{I}_3 - \psi^2\ \bar{I}_5 U^2), \qquad (6)$$

where the shorthand

$$\bar{I}_n \equiv \int_0^1 \left(\frac{c}{c_c}\right)\left(\frac{u}{u_c}\right)^{n-3} d\zeta; \qquad n = 3, 4, 5 \qquad (7)$$

is evaluated, making use of (4) as:

$$\bar{I}_n = \frac{R}{B} + \left[I_n + (I_{n-3} - I_n)\frac{C_A}{C}\right]\left(1 - \frac{R}{B}\right); \qquad n = 3, 4, 5. \qquad (8)$$

Here $I_0 = 1$, $I_1 = 0{\cdot}450$, $I_2 = 0{\cdot}316$ (cf. P1), and $I_3 = 0{\cdot}600$, $I_4 = 0{\cdot}368$, $I_5 = 0{\cdot}278$ are the constant values obtained by evaluating $\bar{I}_3$, $\bar{I}_4$, $\bar{I}_5$ in the ZOEF (i.e. by setting $R = 0$ and $C_A = 0$).

The general solution to eqn (6) is obtained in the Appendix in terms of the centre-line concentration C. The lateral variation of concentration is then obtained from eqn (4). The simplified cases of this general solution are discussed below.

Transport of conservative substances

For conservative substances, let $\gamma = 0$, and for simplicity also let $C_A = 0$ in eqns (A1–A5). With this simplification, note that $Q = 0$, $P = 1$ and $X = 1$ in eqns [A2(b)], (A4) and (A3), and substituting solutions in P1 for B, R and U the centre-line concentration is:

$$C(\xi) = (I_1 - I_2)/[(I_1 - I_4)\mathcal{J}(\xi) + (I_4 - I_2)G(\xi)], \qquad \xi < \xi_s \qquad [9(a)]$$

and

$$C(\xi) = (I_2/I_4)L^{-1/2}(\xi), \qquad \xi > \xi_s, \qquad [9(b)]$$

where the functions $\mathcal{J}$, G and L are given in P1 (eqns B1 and B2 and B4). The various limits in the behaviour of the centre-line concentrations can be investigated in eqns [9(a,b)] by making use of the expressions in P1.

In the case of a constant bottom ($H = 1$), it can be shown that in the ZOFE the centre-line concentration increases with distance for values of the friction parameter $\mu > \mu_c$, where $\mu_c = a(I_4 - I_2)/(I_1 - I_4)$. In the ZOEF the centre-line concentration decreases monotonically with distance and approaches a finite asymptomatic limit

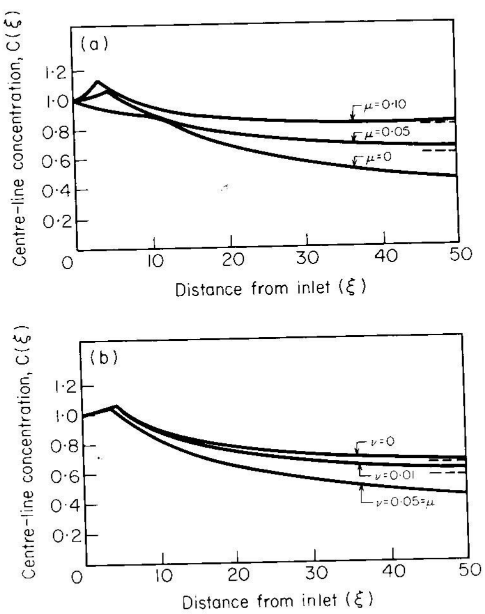

Figure 2. Jet centre-line concentration for (a) constant depth, μ = friction parameter, (b) linearly varying depth, ν = slope parameter.

$C_\infty \equiv I_2/I_4 L_\infty^{1/2}$, where $L_\infty = L(\xi \to \infty)$. The non-vanishing concentration at large distances is a direct result of bottom friction (which reduces advection), but remains an ambiguity in the present solution as the longitudinal diffusion terms have been neglected. The important result of friction is the concentration maximum at some distance from the inlet mouth (within the ZOFE) for $\mu > \mu_c$. For $\mu < \mu_c$ the centre-line concentration decays monotonically with distance, the dependence of which is $\xi^{-1/2}$ when $\mu = 0$. The solutions for the constant depth case are shown in Figure 2(a).

The effect of linear bottom slope (with $H = 1 + \nu\xi$) on the jet concentration is shown in Figure 2(b). Concentration levels decrease with increasing slope due to increased dilution by entrainment, and a non-vanishing centre-line concentration for large distances is again observed in this case when $\mu > 2\nu$.

Transport of suspended sediments

The transport of suspended sediments can be investigated through the general solutions given in the Appendix (for $\gamma \neq 0$) although the behaviour of these analytic solutions is not obvious at first sight since they have to be evaluated numerically.

An equation that complements eqn (1) and represents the bottom deposition rate of suspended sediments within the jet is given by $\partial s/\partial t = S$, where s is the sediment mass per unit area of the bottom. Normalizing, such that $N = s/c_0 h_0$ and $T = u_0 t/b_0$, and utilizing eqns (4) and (5) yields:

$$\frac{\partial N}{\partial T} \equiv K(\xi,\zeta) = \gamma[C_A + (C - C_A)G][1 - \psi^2 F^2 U^2]. \tag{10}$$

Alternatively, the sediment flux (deposition rate) integrated across the jet (normalized by the inlet flux) is given as:

$$K_I(\xi) \equiv \frac{1}{h_0 u_0 c_0} \int_0^b \frac{\partial s}{\partial t} \, dy = B(\xi) \int_0^1 K(\xi.\zeta) \, d\zeta. \quad (11)$$

By virtue of eqn (10), it can be shown that the distribution of the deposition rate across the jet at a fixed distance from the inlet should have two maxima at $\zeta = \pm\zeta_m$ and a minimum at the centre-line. This is a direct result of the competition between the settling (sink) and the lateral diffusion terms in eqn (1). Along the centre-line of the jet, the current velocity is higher; and therefore the settling terms are small. Outside the jet, quiescent conditions exist; the amount of settling is small because it depends only on the

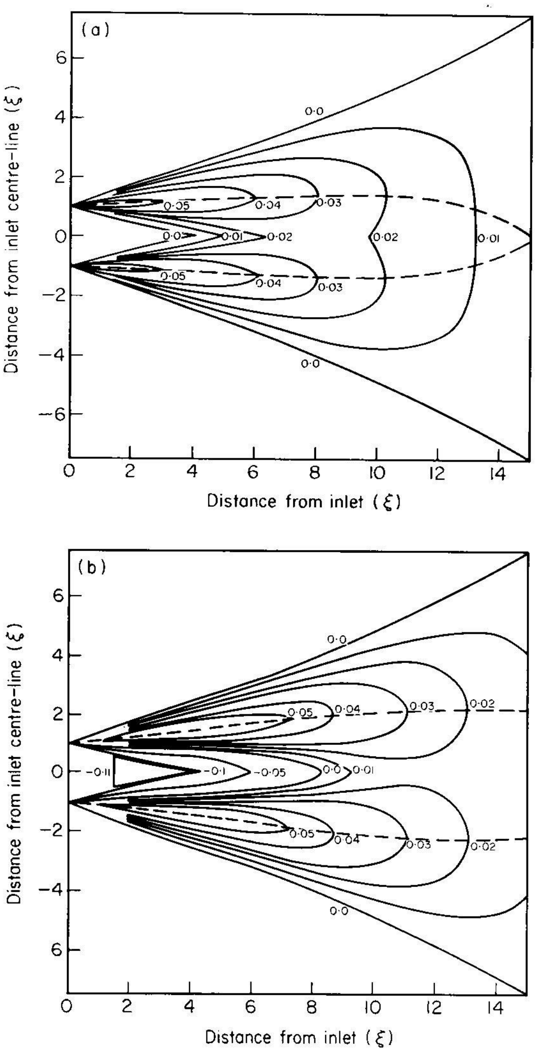

Figure 3. Contours of bottom deposition rate $K(\xi.\ \chi) = K(\xi.B\zeta)$ for (a) $\mu = 0{\cdot}05$, $\nu = 0$, $\gamma = 0{\cdot}1$, $\psi 1{\cdot}0$, and (b) $\mu = 0{\cdot}05$, $\nu = 0$, $\gamma = 0{\cdot}1$, $\psi = 1{\cdot}4$. χ = distance along coast/inlet half-width, ξ = distance offshore/inlet half-width.

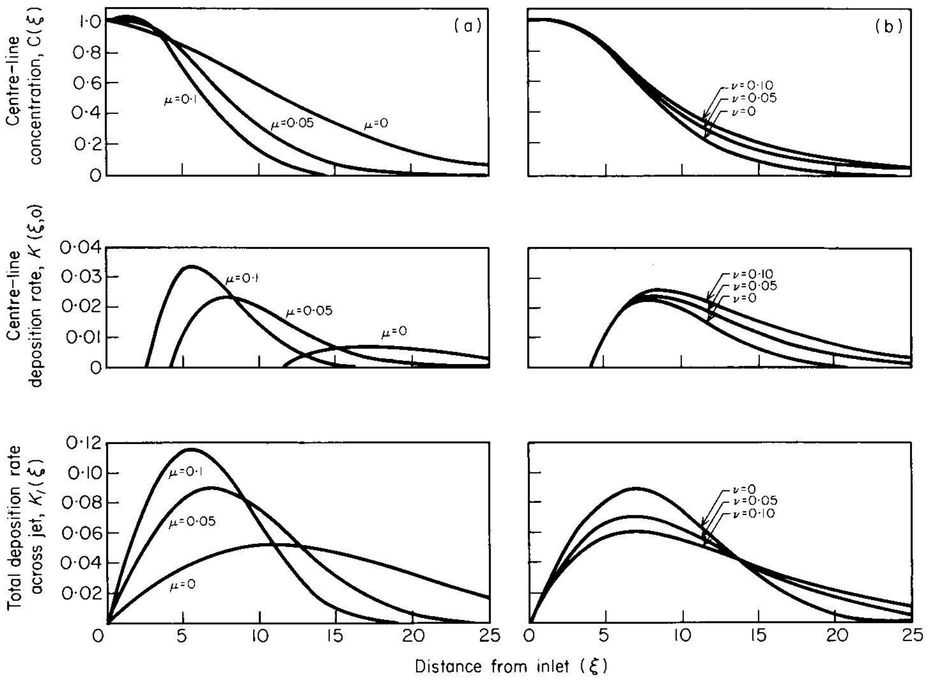

Figure 4(a). Centre-line concentration C, centre-line deposition rate K and integrated deposition rate K_I displaying effects of bottom friction, for μ = variable, $\nu = 0$, $\gamma = 0{\cdot}1$, $\psi = 1{\cdot}0$.
Figure 4(b). As for Fig. 4(a), displaying effects of bottom slope for $\mu = 0{\cdot}05$, υ = variable, $\gamma = 0{\cdot}1$, $\psi = 1{\cdot}0$.

ambient concentration levels. In between, the lateral dependence in eqn (10) indicates maximum settling within the jet at some $|\zeta| = \zeta_m < 1$.

Deposition patterns (contours of $K(\xi,\zeta)$) for two simple cases have been plotted in Fig. 3(a,b) as functions of ξ and $\chi = y/b_0 = B\zeta$. In the first case, the inlet velocity is equal to the critical velocity for settling, $u_0 = u_{cr}$ ($\psi = 1$); and hence there is no settling in the core region of the jet where $u = u_0 = u_{cr}$. There is no settling outside the jet since the ambient concentration is assumed to be zero, $C_A = 0$. Maximum settling occurs at two sides of the jet centre-line where elongated 'marginal shoals' (Oertel, 1975) are usually expected. The loci of maximum settling points ζ_m are shown by dashed line which merge into a single maximum at some distance from the inlet. Along the maximum settling regions the deposition rate decreases in the seaward direction and the initial sharp peaks are flattened. Along the centre-line, maximum depositions are observed at some distance from the mouth where the transversal bar would be expected to build up. In the second case [Figure 3(b)] the velocity at the inlet is 'supercritical' in that u_0 exceeds the critical velocity u_{cr} by 40% ($\psi = 1{\cdot}4$) and hence causes very strong erosion at the mouth and in the core region of the jet where 'inlet troughs' or deep scouring (Oertel, 1975) are usually observed. Postponing further discussion, we note that the settling in the maximum settling regions is also increased as compared to Figure 3(a) since the sediments put into suspension in the erosion region are re-deposited at the further elongated marginal shoals.

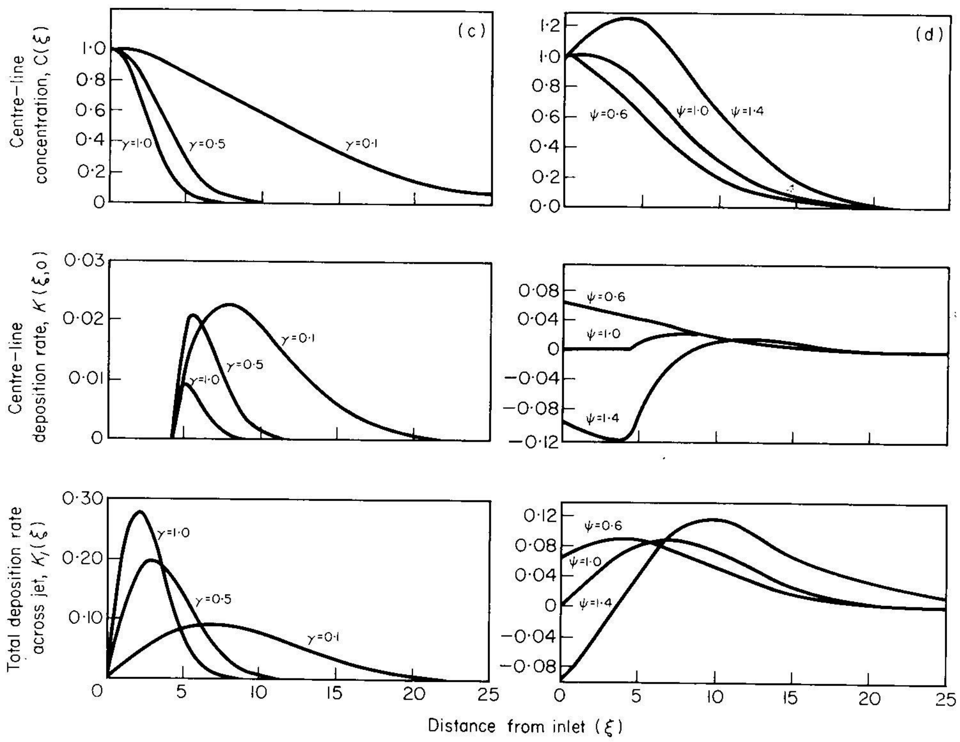

Figure 4(c). As for Fig. 4(a), displaying effects of settling velocity for $\mu = 0{\cdot}05$, $\nu = 0$, γ = variable, $\psi = 1{\cdot}0$.

Figure 4(d). As for Fig. 4(a), displaying effects of inlet velocity for $\mu = 0{\cdot}05$, $\nu = 0$, $\gamma = 0{\cdot}1$, ψ = variable.

Parametric dependence of suspended sediment transport

Bottom friction and topography, sediment settling velocity and the initial velocity at the inlet influence depositional patterns. To investigate the dependence on these factors, results for the jet centre-line concentration $C(\xi)$, the deposition rate at centre-line $K(\xi,0)$, and the total deposition rate integrated across the jet $K_I(\xi)$ [cf. eqns (A5), (10) and (11)] are presented in Figures 4(a–d).

With increasing friction [Figure 4(a)] jet concentrations are reduced more rapidly, resulting in depositions that are closer to the mouth and increased building at the bar crest. The changes in the bottom slope displayed in Figure 4(b) show little influence on either the concentrations or the deposition except that the material is now jetted further offshore and the depositions become more elongated. The effects of sediment settling velocity shown in Figure 4(c) are significant since sediments with larger settling velocities are deposited closer to the inlet, of which the larger proportion goes to the marginal shoals (the centre-line deposition is reduced). This result shows that coarser material will be deposited near the inlet and the marginal shoals, whereas finer material will be jetted further offshore and will be distributed more uniformly yielding a variable sorting around the inlet. The inlet flow conditions, shown in Figure 4(d), also have important consequences with regard to deposition. When an equilibrium discharge is maintained at the inlet with $u = u_{cr}$, no deposition occurs at the mouth or within the jet core [cf. Figure 3(a)]. If the flow velocity is lower than the critical velocity for suspension, large depositions in these zones are expected, which may at times result in the permanent closure of the inlet, through increased friction and bottom build-up. On the other hand, with an over-critical inlet velocity, sediments are brought into suspension at the inlet and the core regions, resulting in intense scouring [cf. Figure 3(b)]. In this case, the material put into suspension at the core region is deposited further offshore in the marginal shoals.

In addition to the above, the effects of ambient concentrations and cross-currents have been included in the analyses by Özsoy (1977), but the details will not be presented here. The ambient concentrations are entrained into the jet and somewhat alter the deposition patterns in which the deposition extends to the quiescent outer region of the jet. For conservative loads, the ambient concentration reduces lateral diffusion; but in the presence of settling, the competition of deposition rates in the inner and outer regions of the jet determines the distribution of concentrations. With cross-currents being present, the centre-line concentration is increased with respect to the straight jet since lateral diffusion is inhibited by the co-flowing component of the cross-current.

Observations and applications

The present model of jet diffusion and suspended sediment transport allows reasonable predictions to be made at tidal inlets under certain conditions. Since direct measurements of diffusion/deposition in a prototype ebb-tidal jet are not available, only qualitative comparisons with observations will be made.

With regard to sedimentation, the genesis of tidal deltas have always puzzled engineers, geologists and oceanographers alike, due to the many factors influencing the shape, volume and building mechanisms of these geomorphic features. While it is generally accepted that reversing tidal currents are mainly responsible in shaping the shoals near an inlet, further variable effects of wave forces, coastal currents, fluvial discharges and storms cannot usually be isolated (Dean & Walton, 1975; Oertel, 1975; Wright & Sonu, 1975; Sonu & Wright, 1975; Hayes & Kana, 1976; Hubbard *et al.*, 1979).

Dean & Walton (1975) noted that wave forces often drive the material deposited by tidal jets back to the shore and therefore limit the shoal volumes. On the other hand, on a low wave energy coast such as the west coast of Florida, large marginal shoals would develop offshore of an inlet. For example, the massive shoals of Boca Grande inlet on the Gulf Coast have the largest depositions in Florida, estimated at 150×10^6 m^3. The shoal bathymetry presented by Dean & Walton of this inlet is in agreement with the model predictions, showing a deep straight channel flanked by two massive marginal shoals. The material entrained into the jet from adjacent shores and those originating from inland sources are deposited until an equilibrium storage form is reached. Oertel (1975) has also noted that the shapes of ebb-tidal deltas are determined by the balance between wave-driven currents and reversing tidal currents at Georgia inlets. The best observed feature of the peripheral shoal complex is the presence of massive marginal shoals which are elongated in the offshore direction when wave influence or littoral currents are less significant. Another feature noted by Oertel is the deep trough located just seaward of the inlet entrance at many instances. These troughs varied in depth from 15 to 30 m below mean sea level and accordingly represented the deepest areas of the coastal waters before the continental shelf dipped to comparable depths. Inlet troughs are possibly formed by deep scouring during extreme flow conditions such as formed by spring tides

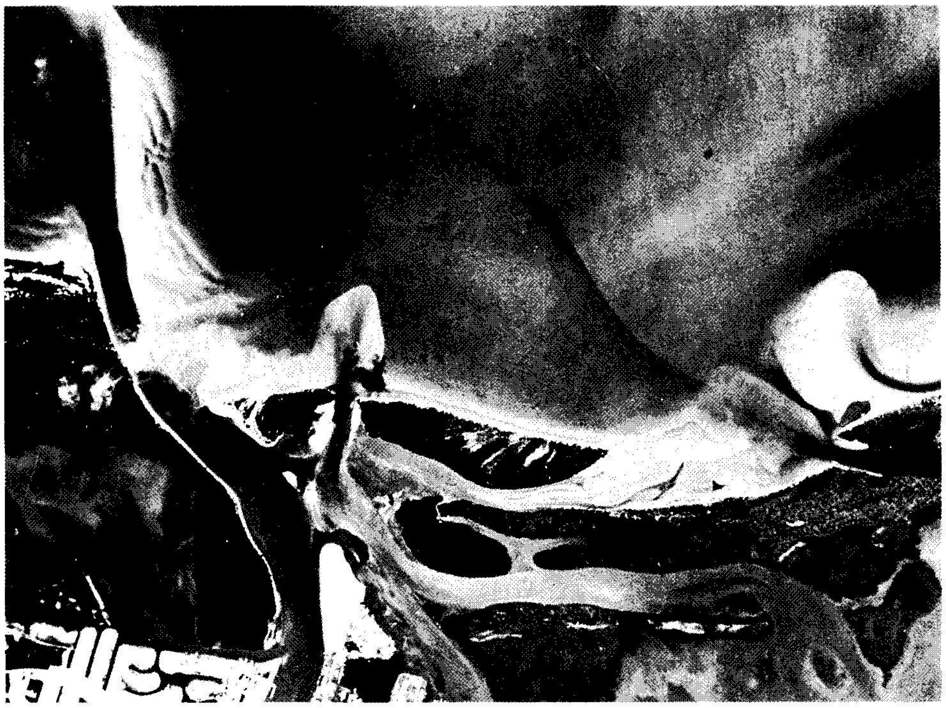

Figure 5. Sediment deposition near four inlets in the vicinity of Big Marco Pass, Marco Island, Florida (courtesy of University of Florida, Coastal Engineering Archives).

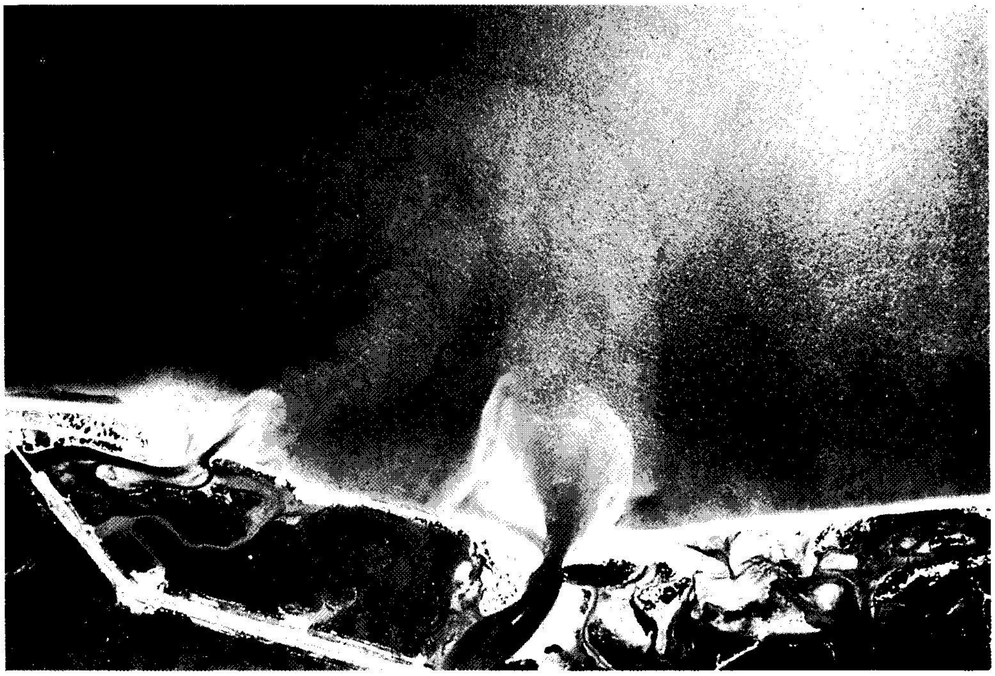

Figure 6. Sediment deposition and jet interaction at New Pass and Big Hickory Pass, Florida (courtesy of University of Florida Coastal Engineering Archives).

or storms. Such erosion within the jet core region is predicted by the present model [Figure 3(b)] when the inlet velocity is higher than critical. During normal (equilibrium) conditions, the inlet velocity should be maintained at the critical level. However, excessive ebb-flow could create a deviation from equilibrium by eroding the channel within the core region and depositing the scour material in the marginal shoals. A similar inlet trough is observed in the bathymetry of Jupiter Inlet (Figure 5 in P1), although this inlet is the smallest of the Florida inlets in terms of its shoal volumes (Dean & Walton, 1975).

Photographical evidence of tidal inlet sedimentation is shown in Figures 5 & 6 for west Florida inlets, where wave influences are minimal. All four inlets in Figure 5 display elongated shoals. In Figure 6, jets issuing from two inlets interact in the offshore region, and similar depositions are seen at the inlets. The jets seem to be attracted to each other through lateral entrainment. The roles of entrainment and sediment trapping are exemplified in Figure 6, since the coastline in between the two nearby jets is indented with

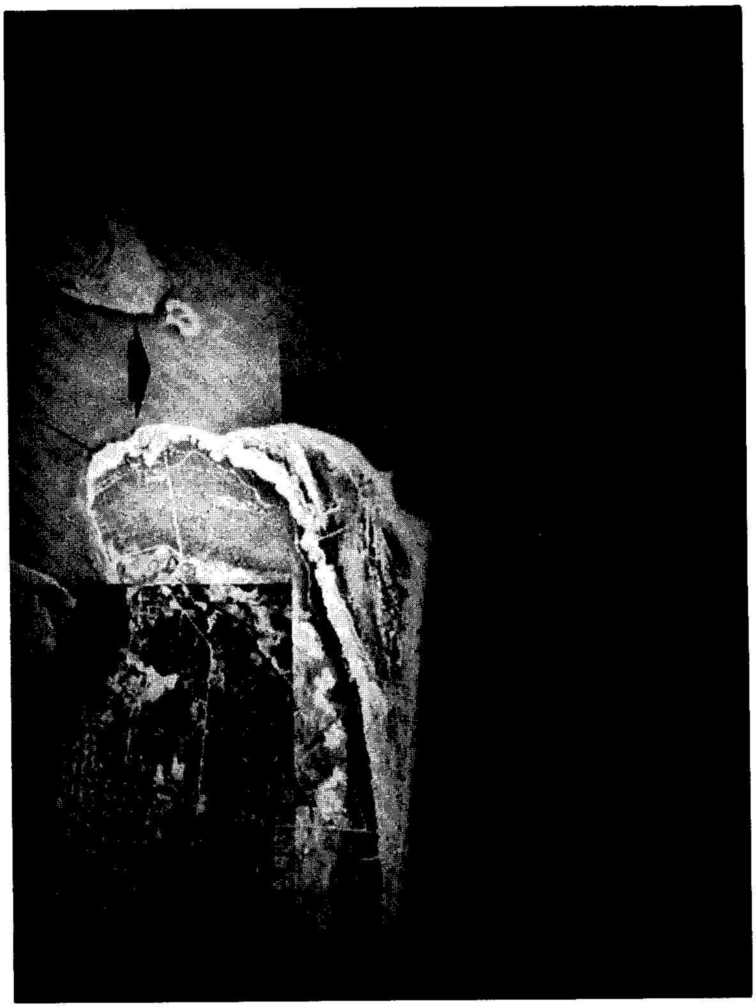

Figure 7. Ebb-flow and entrainment at St. Mary's entrance (courtesy of Eric Olsen, photography date November 1969).

Figure 8. Starting jet at Ponce de Leon Inlet, Florida (courtesy of Volusia Council of Governments, photography date 24 Feb. 1975, No: VCOG–1–23).

respect to the coasts lying on both sides of the inlet pair. The excessive erosion of the intermediate coastline as compared to the outward shores seems to result from continual entrainment of these sands to tidal jets on both sides, which then store the material in the inlet shoals. Another important feature in Figure 6 is the observed migration of the smaller inlet, which is possibly caused by the entrainment of the smaller jet in its relatively larger neighbour.

The role of entrainment is clearly demonstrated in Figure 7. A filament of visible material (probably originating from an outfall to the south) is entrained into the ebb-tidal jet at the tip of the southern jetty. At this inlet, the construction of jetties has led to dramatic alterations in the inlet bathymetry and adjacent coasts. The improved flow at the inlet has caused extensive depositions at the tips of the jetties at the expense of erosion elsewhere in the inlet and on the beaches extending up to 10 km on both of the adjoining coasts. The volume of sediment removed from the littoral system was estimated as 94×10^6 m^3, of which 92×10^6 m^3 was deposited seaward of the jetties (Olsen, 1977).

In Figure 8 the commencement of a tidal jet is indicated by its sediment load in much the same way as Figure 7, (P1). Since the jet is in its initial stage of development, it is in the form of two unsteady vortices trailed by a plug flow (cf. P1). At this particular inlet, the longer north jetty was designed to intercept the southerly longshore transport of sand, which would then be collected in an impoundment basin located on the inlet side of the weir section of the jetty. The alterations that occurred subsequently were drastic, as if to disprove the 'river of sand' (i.e. littoral drift) hypothesis and showed that tidal exchange dominated the morphology rather than littoral drift. The inlet channel migrated towards the impoundment basin and large depositions occurred on the south side, totally covering the south jetty in a period of about five years after the construction (Purpura, 1977). As shown in Figure 8, the north beach eroded dramatically, contrary to expectations. Large depositions occurred offshore of the north jetty and on the south beach. On the basis of tidal hydraulics, this result is not surprising. First, the tidal jet is bent at an oblique angle to the coast by the jetty, while entrainment is allowed through the weir section. Joshi & Taylor (1983) show that entrainment velocities are increased on the obtuse angle side of an oblique jet, which would cause larger erosion on the north beach. Secondly, the presence of a single jetty would create an asymmetrical inlet ebb-flow in the form of a 'wall jet' (Abramovich, 1963). The velocity and concentration profiles adjacent to the solid part of the jetty can be approximated by those corresponding to a half jet (centre-line at jetty), neglecting turbulent transfer near the jetty. The prediction of suspended sediment transport patterns by the present model with centre-line located at the jetty would yield erosion near the jetty and accretion in the shear region on the other side of the inlet (south side), hence the migration of the original channel. Furthermore, secondary circulation within the bending jet would also contribute to this process. Wave diffraction/refraction would result in further evolution. Similar channel migrations have also been noted in other single-jettied inlets (Kieslich & Mason, 1975).

Laboratory investigations of ebb-tidal jets and inlet shoals are very limited, although they are much needed to establish the reliability of any model. Preliminary investigations of equilibrium shoal development in response to tidal jets were reported by Sill *et al.* (1981). Quantitative comparisons with their results are inappropriate since the present model only produces rates of sedimentation and not the equilibrium morphology. It should be noted that, in general, there is a feedback effect in sedimentation since developing shoals would modify the jet hydromechanics through changes in bottom friction and topography. This fact is exemplified by the better agreement of observed features with the model during the initial stages of development. Nevertheless, the 'horseshoe' shaped equilibrium shoals of Sill *et al.* are in qualitative agreement with the model deposition patterns. In the experiments, the final geometry of the shoals was correlated with the empirically obtained inlet current intensity ratio $\psi = u_0/u_{cr}$. No correlation was found with sediment size since the grain sizes used were not varied significantly and were much too large for simulating prototype conditions. It was therefore not clear whether the transport was through suspension or bedload. Finally, the comparison by Sill *et al.* of shoal distribution with the critical velocity isotach, based on the assumption that sediment would accumulate along the isotach, is erroneous. In fact, the model solutions indicate highest rates of deposition in the outer region of the critical velocity isotach [cf. Figure 3(b)], due to the competition between the settling of sediment and the differential rates of lateral sediment and momentum diffusion.

Laboratory experiments on sedimentation at river mouths can also be used for comparison with the model since the experimental conditions reported are much similar to the ebb-tidal jet, i.e. steady or quasi-steady river flow without buoyancy effects. For example, Shemdin (1969) modelled bed changes occurring near a river mouth before and after a flood. Although the sediments were not introduced by the river, the erosion at the jet core produced by flood conditions and the subsequent deposition at the marginal shoals resulted in ‘ tear-drop ’ deposition patterns which were strikingly similar to those predicted by the present model [Figure 3(b)]. Physical model studies by Butakov (1971) also showed deposition patterns with two marginal sand banks which joined together at some distance away from the mouth [quite similar to that of Figure 3(a)]. At later stages of development, the increased height of the transversal bar increased friction and resulted in a widening of the depositions. Mikhailov (1972) also reports experiments in which similar results were obtained. In addition, it was observed that the rate of deposition was inversely proportional to bottom slope [cf. Figure 4(b)] and that the increased building of a transversal bar can result in the bifurcation of the flow. These experiments however, were, not carefully controlled, since they were not guided by a particular model of sediment transport. However, it is interesting to note that Butakov (1971) made a rather crude attempt to model bed-load transport by a jet and was able to calculate bar building rates with patterns similar to his experiments and the present results.

Some numerical experiments of sedimentation at river mouths were made by Bonham–Carter & Sutherland (1967). While the diffusion of momentum was modelled as a turbulent jet, turbulent diffusion of suspended sediments in the jet was not considered. Because of this deficiency of the model and since the jet was not in touch with the bottom, the resulting depositions were approximately uniform within the fan. Numerical experiments on river delta sedimentation were later detailed by Farmer & Waldrop (1977), who used the turbulent momentum and diffusion equations including sediment settling and resuspension from the bottom. They were successful in simulating bar building and scouring at the river mouth.

Although the present model is not applicable to river plumes in general due to buoyancy effects, some similarity is found in nature, as noted in the above experiments. The model may find limited application in the initial part of river plumes (within a few river widths distance), especially during high floods and before buoyant spreading causes separation from the bottom. It is worthy of note, however, that rivers with significant momentum and sediment fluxes display very similar depositional features to those predicted. It was noted by Mikhailov (1972) that the seaward advance of a delta and extension of river channels occur principally in bar areas. The extensive review by Wright & Coleman (1974) also showed that the embankments of the Mississippi delta channels progressed through the building of ‘ sub-aqueous levees ’ which then became exposed. In fact, the sub-aqueous levees can be formed in much the same way as the marginal shoals of a tidal inlet, i.e. by the competition between lateral diffusion and settling in a jet. The only explanation advanced for these features by Wright & Coleman (1974) was the presence of secondary circulations (also simulated by Farmer & Waldrop, 1977) in a buoyant plume.

The main results of the model are summarized as follows:

(1) The ebb-tidal transport processes can be represented by a turbulent jet in which diffusion is modified by settling of suspensions.
(2) Bottom friction decreases the rate of dilution in the jet through entrainment and can result in a maximum in the core region. On a sloping bottom, increased entrainment flux counteracts with frictional effects. Ambient currents and concentrations also influence the diffusion pattern.
(3) Sediment concentrations in the jet decay through deposition at the bottom, which occurs mainly at lateral lobes. The pattern of deposition depends on bottom friction and slope, the inlet current intensity, and size of sediment. Sediments including different sizes become sorted upon deposition.

Conclusions

In spite of the major environmental and engineering concerns associated with numerous tidal entrances around the world, a full understanding of their hydromechanics has not been reached at present. A diverse set of environmental processes which varies from one tidal inlet to the next influences the hydraulics, mixing and transport characteristics, geomorphology and stability of these economically important regions. The relative importance of each physical process and interactions between different processes could not be resolved in the past and, therefore, empirical descriptions have often been advanced.

With regard to the transport and sedimentation processes, some of the basic tidal mechanisms have at times been overlooked in the past and too much emphasis has often been placed on the littoral processes. While littoral processes are certainly of importance, detailed models of tidal hydromechanics are at least equally justified in supplying some of the basic ingredients in the puzzle. In a series of articles (Özsoy & Ünlüata, 1982; Joshi & Taylor, 1981; this paper) tidal effects have been further elaborated, based on earlier conceptual developments. The emphasis placed on tidal hydromechanics is rooted in the fact that the tide constitutes a persistent (diurnal or semi-diurnal) signal, whereas the climatological signals are highly variable and are only effective in the average sense. The residual circulations even in the far-field were found to be significant and to the same order of magnitude as the littoral drift estimates by Joshi & Taylor (1981). However, the material raised into suspension in the littoral zone is of importance in initiating transport. The sediments supplied by littoral processes are then entrained into the tidal residual circulation and finally deposited in tidal inlet shoals, where the importance of tidal mechanisms rises sharply.

The present model can be used to make reasonable qualitative predictions with regard to certain aspects of the transport processes and opens up new prospects in understanding tidal inlets. However, the subject is also open for further development, testing of hypotheses and experimental verification.

References

Abramovich, G. N. 1963 *The Theory of Turbulent Jets*. M.I.T. Press, Cambridge, Mass.
Ariathurai, R. & Krone, R. B. 1976. Finite element model for cohesive sediment transport. *Journal of the Hydraulics Division, American Society of Civil Engineers*, **102**(HY3), 323–338.

Bonham-Carter, G. F. & Sutherland, A. J. 1967 Diffusion and settling of sediments at river mouths: A computer simulation model. *Transactions of the Gulf Coast Association of Geological Societies*, **17**, 326–338.

Bruun, P. (ed.) 1978 *Stability of Tidal Inlets*. Elsevier, Amsterdam. 510 pp.

Butakov, A. N. 1971 Study of development and deformation of mouth bar. *14th Congress of the IAHR*, **4**, No. D-12, pp. 92–102.

Cormault, P. 1971 Determination experimentale du debit solide d'erosion de sediments fins cohesifs. *14th Congress of the IAHR*, **4**, No. D-2, pp. 9–16.

Dean, R. G. & Walton, T. L. 1975 Sediment transport processes in the vicinity of inlets with special reference to sand trapping. In *Estuarine Research* (Cronin, L. E., ed.). Academic Press, New York. **2**, 129–149.

Farmer, R. C. & Waldrop, W. R. 1977 A model for sediment transport and delta formation. *Coastal Sediments 77. 5th Symposium of the Waterway, Port, Coastal and Ocean Division, ASCE*, pp. 102–115.

French, J. L. 1960 Tidal flow in entrances. U.S. Army Corps of Engineers, Committee on Tidal Hydraulics, Technical Bulletin No. 3.

Hayes, M. O. & Kana, T. W. 1976 Terrigeneous clastic depositional environments. University of South Carolina, Technical Report No. 11-CRD.

Hubbard, D. K., Oertel, G. & Nummedal, D. 1979 The role of waves and tidal currents in the development of tidal-inlet sedimentary structures and sand body geometry: Examples from North Carolina, South Carolina and Georgia. *Journal of Sedimentary Petrology*, **49**(4), 1073–1092.

Joshi, P. B. 1982 Hydromechanics of tidal jets. *Journal of the Waterways, Port, Coastal and Ocean Division, American Society of Civil Engineers*, **103**(WW3), 239–253.

Joshi, P. B. & Taylor, R. B. 1983 Circulation induced by tidal jets. *Journal of the Waterways, Port, Coastal and Ocean Division, American Society of Civil Engineers*, **109**(4), 445–464.

Kieslich, J. M. & Mason, C. 1975 Channel entrance response to jetty construction. *Proceedings of the Civil Engineering in the Oceans III Conference*, Newark, Delaware, 689–705.

Mehta, A. J. & Özsoy, E. 1978 Flow dynamics and nearshore transport. In *Stability of Tidal Inlets: Theory and Engineering* (Bruun, P., ed.). Elsevier, New York. pp. 83–161.

Mehta, A. J. & Zeh, T. S. 1980 Influence of a small inlet in a large bay. *Coastal Engineering*, **4**, 157–176.

Mikhailov, V. N. 1972 Hydrology and formation of river-mouth bars. In *Spits and Bars*. Dowden, Hutchinson and Ross Inc., Stroudsberg, Pennsylvania.

Nihoul, J. C. J. (ed.) 1975 *Modelling of Marine Systems*. Elsevier, New York.

Nihoul, J. C. J. & Adam, Y. 1975 Dispersion and settling around a waste disposal point in a shallow sea. *Journal of Hydraulic Research*, **13**, 171–186.

O'Brien, M. P. & Dean, R. G. 1972 Hydraulic and sedimentary stability of coastal inlets. *Proceedings of the 13th Coastal Engineering Conference*, p. 761.

Odd, N. V. M. & Owen, M. W. 1972 A two layer model of mud transport in the Thames estuary. *Proceedings of the Institution of Civil Engineers* **7517** (Suppl.), 175–205.

Oertel, G. F. 1975 Ebb-tidal deltas of Georgia estuaries. In *Estuarine Research* (Cronin, L. E., ed.). Vol. 2. Academic Press, New York. 267–276.

Officer, C. B. 1976 *Physical Oceanography of Estuaries*. John Wiley and Sons, New York.

Olsen, E. 1977 A study of the effects of inlet stabilization at St. Marys entrance, Florida. *Coastal Sediments 77, 5th Symposium of the Waterway, Port, Coastal and Ocean Division, ASCE*, pp. 311–329.

Özsoy, E. 1977 Flow and mass transport in the vicinity of tidal inlets. Coastal and Oceanographic Engineering Laboratory, University of Florida, Report No. TR-036, 196 pp.

Özsoy, E. & Ünlüata, Ü 1982 Ebb-tidal flow characteristics near inlets. *Estuarine, Coastal and Shelf Science*, **14**, 251–263.

Purpura, J. A. 1977 Performance of a jetty-weir inlet improvement plan. *Coastal Sediments 77, 5th Symposium of the Waterway, Port, Coastal and Ocean Division, ASCE*, pp. 330–349.

Schlichting, H. 1968 *Boundary Layer Theory*, 6th ed. McGraw Hill, New York.

Shemdin, O. H. 1969 Interaction of a river with the coast: laboratory simulation. *Proceedings of the Civil Engineering in the Oceans II Conference*, Miami Beach, Florida, 763–782.

Sill, B. L., Fisher, J. S. & Whiteside, S. D. 1981 Laboratory investigation of ebb-tidal shoals. *Journal of the Waterways, Port, Coastal and Ocean Division, American Society of Civil Engineers* **107**(WW4), 233–242.

Sonu, C. J. & Wright, L. D. 1975 Mass transport and dispersion off a tidal inlet. Offshore Technology Conference, Paper No. OTC 2383.

Stolzenbach, K. D. & Harleman, D. R. F. 1971 An analytical and experimental investigation of surface discharges of heated water. Ralph M. Parsons Laboratory for Water Resources and Hydrodynamics, M.I.T., Report No. 135.

Taylor, R. D. & Dean, R. G. 1974 Exchange characteristics of tidal inlets. *Proceedings of the 14th Coastal Engineering Conference*, pp. 2268–2289.

Taylor, R. B. & Joshi, P. B. 1979 Continental shelf circulation induced by tidal jets, an analytical study. Tetra Tech Inc., Report No TC 3249, 108 pp.

Wang, J. D. & Connor, J. J. 1975 Mathematical Modeling of Near Coastal Circulation. Ralph M. Parsons Laboratory for Water Resources and Hydrodynamics, M.I.T., Report No. 200.

Wright, L. D. & Coleman, J. M. 1974 Mississippi River mouth processes: effluent dynamics and morphologic development. *Journal of Geology*, **82**, 751–778.
Wright, L. D. & Sonu, C. J. 1975 Processes of sediment transport and tidal delta development in a stratified tidal inlet. In *Estuarine Research* (Cronin, L. E., ed.). Academic Press, New York. **2**, 63–76.

Appendix

In order to solve the ordinary differential equation (6) for concentration $C(\xi)$, first equation (8) are substituted, then by rearranging the equation it is put into the form:

$$\frac{dX}{d\xi}+Q(\xi)X=M(\xi), \tag{A1}$$

where

$$X(\xi)\equiv(I_1-I_4)(B-R)HUC_A+[R+I_4(B-R)]HUC, \quad [A2(a)]$$

$$Q(\xi)\equiv\frac{\gamma[R+I_3(B-R)]-\gamma\psi^2U^2[R+I_5(B-R)]}{HU[R+I_4(B-R)]}, \quad [A2(b)]$$

$$M(\xi)\equiv aHUC_A+\gamma[\psi^2U^2(I_2-I_5)-(1-I_3)](B-R)C_A+(I_1-I_4)HU(B-R)C_AQ(\xi), \quad [A2(c)]$$

with the caution that one must set $U=1$ in the ZOFE and $R=0$ in the ZOEF. The functions B, R, U are to be obtained from solutions in P1 for given μ and $H(\xi)$, and $C_A(\xi)$ is the prescribed ambient concentration.

The initial conditions at the inlet mouth are $H(0)=R(0)=B(0)=C(0)=1$, so that $X(0)=1$. Integration of equation (A1) yields

$$X(\xi)=\frac{1}{P(\xi)}\left\{\int_0^{\xi} P(\xi')M(\xi')d\xi'+1\right\}, \tag{A3}$$

where $P(\xi)$ is an integration factor:

$$P(\xi)\equiv\exp\int_0^{\xi} Q(\xi')\ d\xi'. \tag{A4}$$

Therefore, the centre-line concentration is obtained from [A2(a)] as:

$$C(\xi)=\frac{X(\xi)-(I_1-I_4)HU(B-R)C_A}{[R+I_4(B-R)]HU}. \tag{A5}$$

Note that one needs to set $U=1$ in the ZOFE ($\xi<\xi_s$), and $R=0$ in the ZOEF ($\xi>\xi_s$) when making use of the solution (A5).